Cell Reports, Volume *24*

Supplemental Information

B-Cell-Intrinsic Type 1 Interferon Signaling Is Crucial for Loss of Tolerance and the Development of Autoreactive B Cells

Phillip P. Domeier, Sathi Babu Chodisetti, Stephanie L. Schell, Yuka Imamura Kawasawa, Melinda J. Fasnacht, Chetna Soni, and Ziaur S.M. Rahman

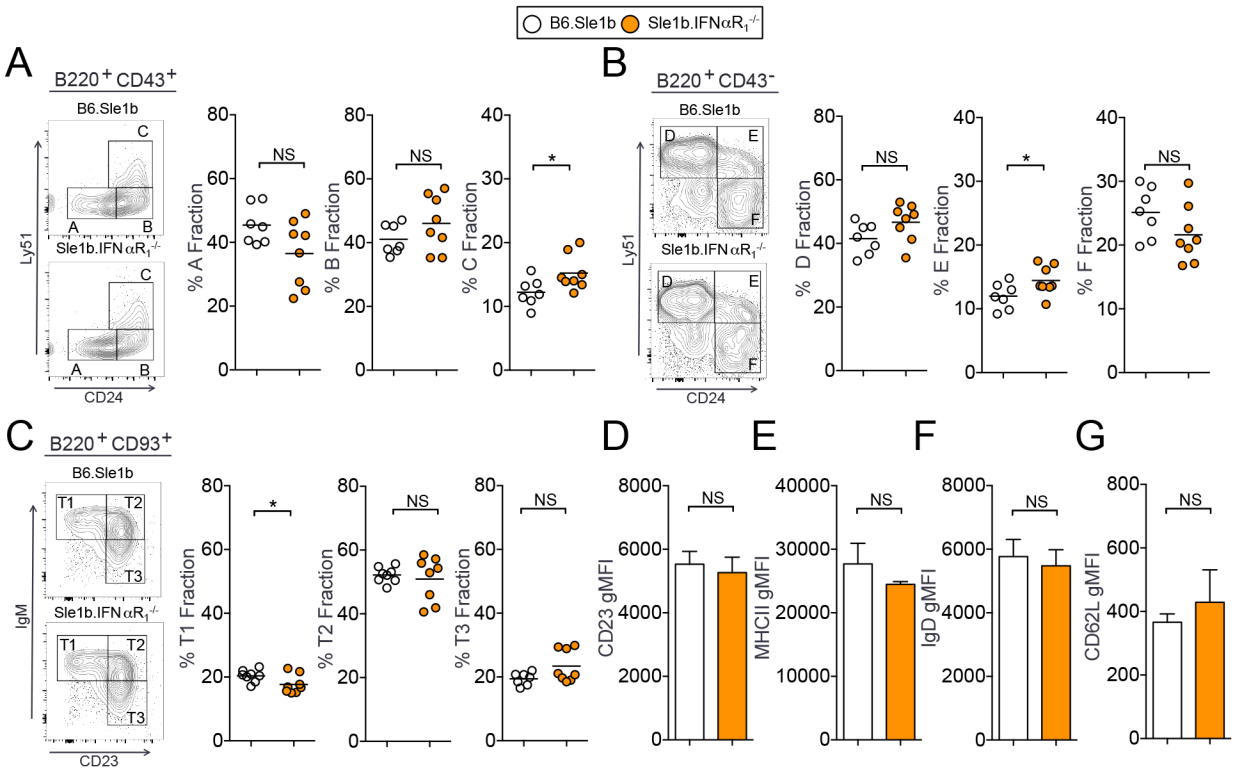

Figure S1. IFNαR1 signaling does not overtly affect B cell development. *Related to Figure 1.*

(A-B) Flow cytometric analysis of bone marrow cells for B cell developmental fractions A ($B220^+CD43^+CD24^-Ly\text{-}51^-$), B ($B220^+CD43^+CD24^+Ly\text{-}51^-$), C ($B220^+CD43^+CD24^+Ly\text{-}51^+$), D ($B220^+CD43^-CD93^+IgM^-$), E ($B220^+CD43^-CD93^+IgM^+$) and F ($B220^+CD43^-CD93^-IgM^+$). (C) Flow cytometric analysis of total splenocytes for B cell developmental stages such as T1 ($B220^+CD93^+CD23^-IgM^+$), T2 ($B220^+CD93^+CD23^+IgM^+$) and T3 ($B220^+CD93^+CD23^+IgM^{low}$). (D-G) Flow cytometric analysis of surface expression of CD23 (D), MHCII (E), IgD (F), and CD62L (G) on total $B220^+$ splenocytes. For A-C, each symbol represents a mouse and horizontal lines indicate mean values. For D-G, bars indicate mean gMFI values ± SD for at least 3 mice per group. Statistical significance was determined using an unpaired, nonparametric Mann-Whitney Student's *t*-test (*, $p < 0.05$, NS, not significant).

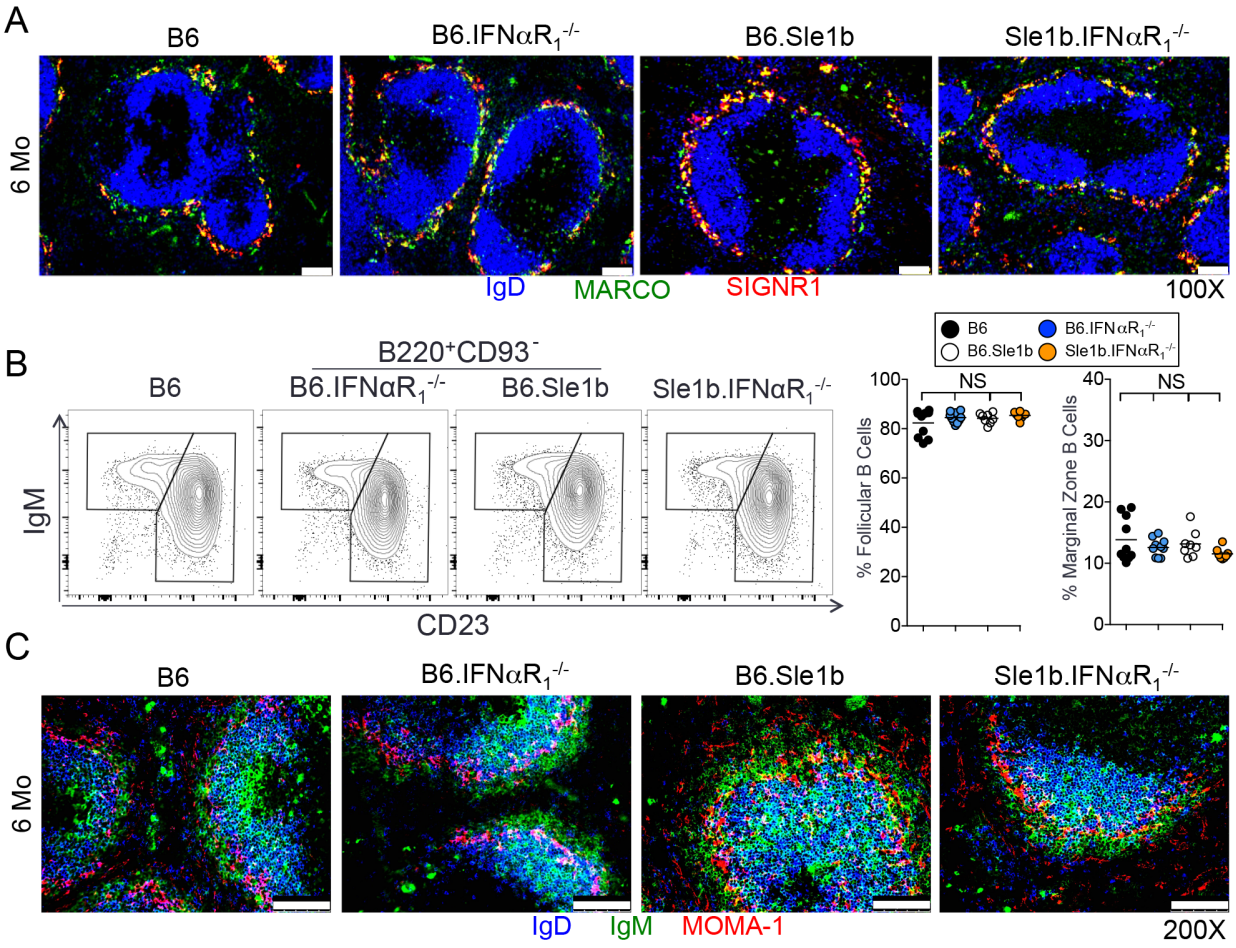

Figure S2. IFNαR1 signaling does not regulate the MZ compartment in B6.*Sle1b* mice. *Related to Figures 1 and 2.*

(A) Representative spleen sections from 6 mo old female mice of the indicated genotypes were stained with anti-IgD (blue), anti-MARCO (green) and anti-SIGNR1 (red) to show $MARCO^{+}SIGNR1^{+}$ marginal zone macrophage (MZM) compartment. Bars, 100 μM. (B) Flow cytometric analysis of total splenocytes to quantitate the percentage of follicular ($B220^{+}CD23^{+}CD93^{-}IgM^{int}$) and marginal zone ($B220^{+}$ $CD23^{-}CD93^{-}IgM^{hi}$) B cells. Each symbol represents a mouse and horizontal lines indicate mean values. Statistical significance was determined using an unpaired, nonparametric Mann-Whitney Student's t test (NS, not significant). (C) Representative spleen sections from 6 mo old female mice of the indicated genotypes were stained with anti-IgD (blue), anti-IgM (green) and anti-MOMA-1 (red) to show marginal zone compartment ($IgD^{-}IgM^{hi}$) structures. Bars, 100 μM.

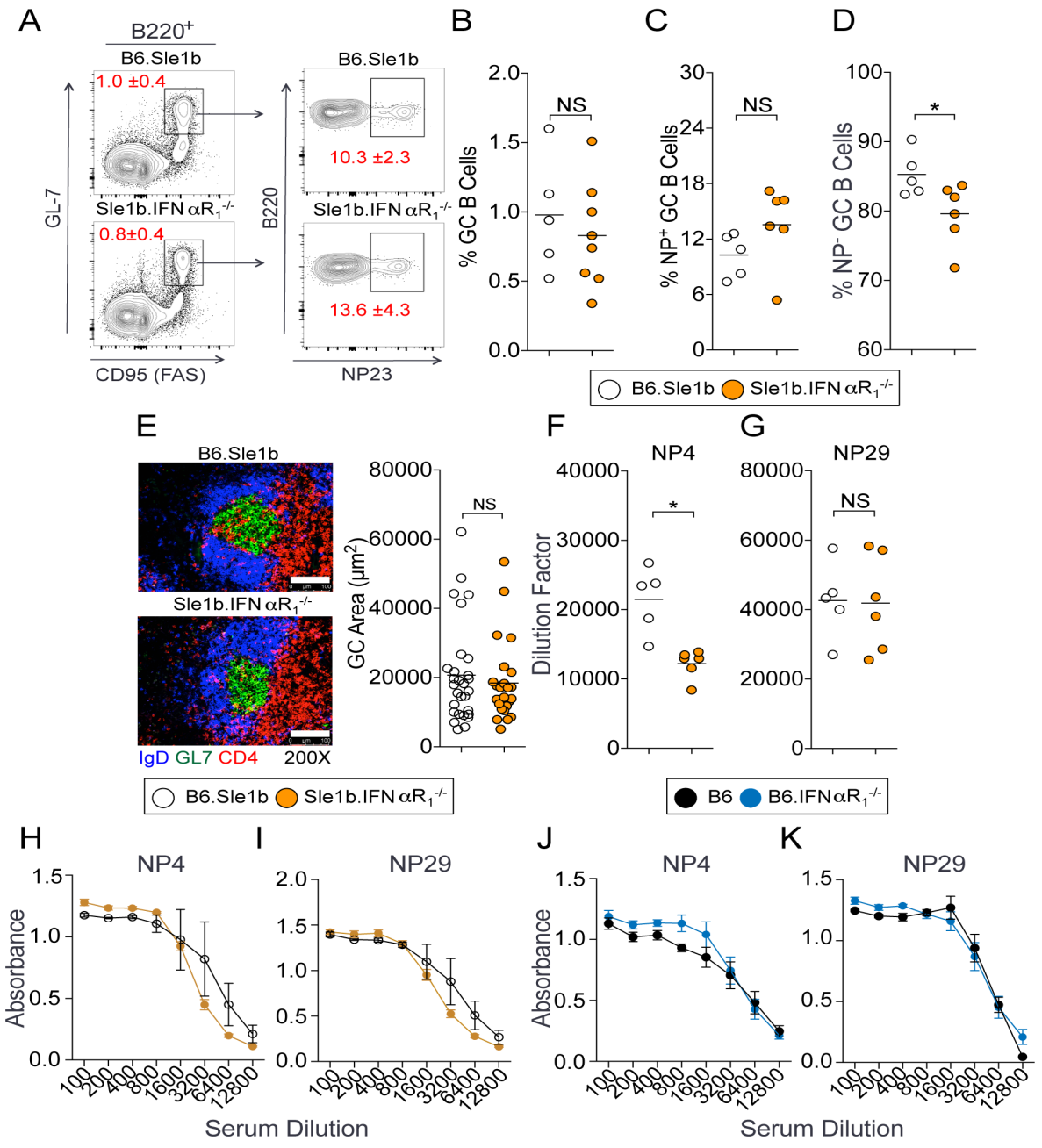

Figure S3. IFNαR1 is not required for high affinity antibody production in B6.*Sle1b* mice over time. *Related to Figures 1 and 2.*

(A and B) B6.*Sle1b* and B6.*Sle1b*.IFNαR1$^{-/-}$ mice were immunized with NP-CGG. Flow cytometric analysis was performed at 14d post-immunization to quantitate the percentage of total B220^{+}GL-7^{hi}Fas^{hi} GC B cells (A left panel and B), NP^{+}B220^{+}GL-7^{hi}Fas^{hi} GC B cells (A right panel and C) and NP^{-}B220^{+}GL-7^{hi}Fas^{hi} GC B cells (D). E- left panels, spleen sections from these mice were stained with anti-IgD (blue), GL7 (green) and anti-CD4 (red). Bars, 100 μM. E-right panels, GC areas were measured in stained spleen secrions. Analysis of NP4- (F, H) and NP29-specific (G, I) serum IgG titers in B6.*Sle1b* and B6.*Sle1b*.IFNαR1$^{-/-}$ mice 14d and 30d post-NP-CGG immunization. Analysis of NP4- (J) and NP29-specific (K) IgG titers in B6 and B6.IFNαR1$^{-/-}$ mice 30d post-NP-CGG immunization. Each symbol represents a mouse and horizontal lines indicate mean values. Statistical significance was determined using an unpaired, nonparametric Mann-Whitney Student's *t*-test (NS, not significant, *, p<0.05).

Supplemental Table 1.

Ingenuity Canonical Pathways	-log(p-value)	Ratio	Molecules
Cytokine/Chemokine Pathways			
IL-2 Signaling	1.310	0.063	PIK3R3,STAT5A,FRS2,IL2RG
IL-3 Signaling	2.680	0.084	PIK3R3,INPP5D,STAT1,STAT5A,FRS2,PPP3CB,PPP3CA
IL-4 Signaling	2.510	0.079	NFATC3,PIK3R3,INPP5D,HLA-DQB1,FRS2,IL4R,IL2RG
IL-9 Signaling	3.410	0.133	NFKB1,PIK3R3,STAT1,STAT5A,FRS2,IL2RG
IL-10 Signaling	1.230	0.059	NFKB1,IL10RB,IL18RAP,IL4R
IL-15 Signaling	1.620	0.066	NFKB1,PIK3R3,STAT5A,FRS2,IL2RG
IL-22 Signaling	1.840	0.125	IL10RB,STAT1,STAT5A
B Cell Activating Factor Signaling	1.260	0.075	NFATC3,NFKB1,MAP3K1
Interferon Signaling	1.380	0.083	IFNAR2,STAT1,IFNAR1
Integrin Signaling	0.991	0.037	ARPC2,PIK3R3,CAPN5,FRS2,TSPAN5,PIKFYVE,CRK,CAPN7
CXCR4 Signaling	0.419	0.012	GNG5,KL
Costimulation			
iCOS-iCOSL Signaling in T Helper Cells	3.500	0.082	NFATC3,GRAP2,NFKB1,PIK3R3,INPP5D,HLA-DQB1,FRS2,PPP3CB,PPP3CA,IL2RG
BCR Signaling			
B Cell Receptor Signaling	1.720	0.049	NFATC3,NFKB1,PIK3R3,INPP5D,MAP3K1,FRS2,PPP3CB,PPP3CA,MEF2C
PI3K Signaling in B Lymphocytes	1.230	0.047	NFATC3,NFKB1,INPP5D,PPP3CB,IL4R,PPP3CA
Calcium Signaling	0.729	0.034	NFATC3,PPP3CB,MYH10,PPP3CA,PRKACB,MEF2C
PTEN Signaling	0.976	0.017	SHARPIN,CDKN1B
Cellular Pathways			
Apoptosis Signaling	0.900	0.045	NFKB1,CAPN5,CAPN7,CASP8
Autophagy	1.080	0.033	ATG4C,CTSH
Actin Cytoskeleton Signaling	0.653	0.031	ARPC2,PIK3R3,FN1,FRS2,MYH10,PIKFYVE,CRK
Glycogen Degradation III	1.620	0.071	MGAM
Cdc42 Signaling	1.460	0.012	CD3D,LIMK1
Transcription Factors			
NF-κB Signaling	1.020	0.039	EIF2AK2,NFKB1,PIK3R3,MAP3K1,FRS2,PRKACB,CASP8
Disease Associated Pathways			
Systemic Lupus Erythematosus Signaling	0.272	0.022	NFATC3,PIK3R3,LSM6,INPP5D,FRS2

Table S1. *Ingenuity Canonical Pathway Analysis* of B6.*Sle1b* and B6.*Sle1b*.IFNαR$_1^{-/-}$ non-GC and GC B cells. *Related to Figure 5.*

Differentially expressed genes shown in Figure 5A were processed by *Ingenuity Pathway Analysis*. Representative canonical pathways as identified by *Ingenuity* software are shown for differentially expressed genes.

Supplemental Experimental Procedures

RNA Sequencing

$B220^{+}Fas^{hi}PNA^{hi}$ spontaneous GC B cells and $B220^{+}Fas^{low}PNA^{low}$ non-GC B cells from the indicated mouse strains were sorted with a FACS Aria Sorter (BD Biosciences). RNA was extracted from sorted cells by TRIzol as per the manufacturer's instructions (Ambion, Grand Island, NY). Optical density values of extracted RNA were measured using NanoDrop (Thermo Fisher Scientific, Waltham, MA) to confirm an A260:A280 ratio above 1.9. RNA integrity number (RIN) was measured using BioAnalyzer (Agilent Technologies, Santa Clara, CA) RNA 6000 Pico Kit to confirm RIN above 7. The cDNA libraries were prepared using the Ovation RNA-seq System V2 (NuGEN, San Carlos, CA) as per the manufacturer's instructions. The unique barcode sequences were incorporated in the adaptors for multiplexed high-throughput sequencing. The final product was assessed for its size distribution and concentration using BioAnalyzer High Sensitivity DNA Kit (Agilent Technologies) and then loaded onto TruSeq SR v3 flow cells on an Illumina HiSeq 2500 (Illumina, San Diego, CA) and run for 100 cycles using a paired-read recipe (TruSeq SBS Kit v3, Illumina) according to the manufacturer's instructions. Illumina CASAVA pipeline (released version 1.8, Illumina) was used to obtain de-multiplexed sequencing reads (fastq files) passed the default purify filter. Additional quality filtering used FASTX-Toolkit (http://hannonlab.cshl.edu/fastx_toolkit) to keep only reads that have at least 80% of bases with a quality score of 20 or more (conducted by fastq_quality_filter function) and reads left with 10 bases or longer after being end-trimmed with a base quality score of 20 (conducted by fastq_quality_trimmer function). A bowtie2 index was built for the mouse reference genome (GRCm38) using bowtie version 2.1.0. The RNA-seq reads of each of the 38 samples were mapped using Tophat version 2.0.9 (Trapnell and Salzberg, 2009) supplied by Ensembl annotation file; GRCm38.78.gtf. Gene expression values were computed using fragments per kilo base per million mapped reads (FPKM) values. Differential gene expression was determined using Cuffdiff tool which is available in Cufflinks version 2.2.1 (Trapnell et al., 2010) supplied by GRCm38.78.gtf. Normalization was performed via the median of the geometric means of fragment counts across all libraries, as described in (Anders and Huber, 2010). Statistical significance was assessed using a false discovery rate (FDR) threshold of 0.05. Genes that were expressed at $\geq$ 2-fold differences between GC B cells and non-GC B cells were sorted by hierarchical clustering using Cluster 3.0 software (Version 1.54) and heatmaps were generated using TreeView software (Version 1.1 6r4) (Saldanha, 2004).

Flow cytometry

Flow cytometric analysis of mouse splenocytes or bone marrow cells was performed using the following antibodies: PacBlue-anti-B220 (RA3-6B2); Alexa Fluor 700-anti-CD4 (RM4-5); PE-anti-PD-1 (29F.1A12); Cy5-anti-CD86 (GL1); PeCy7-anti-CD95 (FAS, Jo2); PeCy7-anti-MHC-II (M5/114.15.2); APC-anti-CD24 (HSA) (M1/69); Biotin-anti-Ly5.1 (BP-1) (6C3); FITC-anti-CD23 (B3B4) and PE-Cy5-streptavidin (SA) were purchased from BioLegend, San Diego, CA. Biotin-anti-CXCR5 (2G8) from BD Pharmingen, San Diego, CA. FITC-peanut agglutinin (PNA) from Vector Labs, Burlingame, CA. PE-anti-IgM (eB121-15F9); APC anti-CD93 (AA4.1); FITC-anti-F4/80 (BM8) from eBiosciences, San Diego, CA. Stained cells were analyzed using the BD LSR II flow cytometer (BD Biosciences, Franklin lakes, NJ). Data were acquired using FACSDiva software (BD Biosciences, San Jose, CA) and analyzed using FlowJo software (Tree Star, San Carlos, CA).

Immunohistology

Immunohistochemical analysis of mouse spleen sections was performed using the following antibodies and reagents: PE-anti-CD4 (GK1.5); FITC-GL7; APC-anti-IgD (11-26c.2a) (all from BD Biosciences); SIGNR1 (hamster Ab-eBioscience; clone ebio22D1); MOMA-1 (Abcam, Cambridge, MA); E4-biotin (made in house); Strepavidin-PE (Sigma Aldrich, St. Louis, MO). Spleen cryostat sections (5-6 um) were prepared as previously described (Wong et al., 2012). Immunohistochemistry was performed as described (Wong et al., 2012) and stained sections were analyzed with a Leica DM4000 fluorescence microscope and Leica software (Leica Microsystems, Buffalo Grove, IL). The color intensity of the images was slightly enhanced using Adobe Photoshop CS4 (Adobe Systems, San Jose, CA) for better visualization. These color enhancements were carried out consistently between all sections while maintaining the integrity of the data. Biotin-anti-E4 was generated in house.

Quantification of germinal center frequency and areas by histology

Immunohistochemistry was performed using the Abs listed in the Immunohistology methods. Images of stained sections were captured using a Leica DM4000 fluorescence microscope and Leica software (Leica Microsystems, Buffalo Grove, IL). To determine the GC frequency, total GC numbers were quantitated in 5 separate 10X field areas per spleen section. For the GC area and fluorescence intensity measurements, 10 GCs/mouse were measured using the LASAF software package.

Supplemental References

Anders, S., and Huber, W. (2010). Differential expression analysis for sequence count data. Genome Biol *11*, R106.
Saldanha, A.J. (2004). Java Treeview--extensible visualization of microarray data. Bioinformatics *20*, 3246-3248.
Trapnell, C., and Salzberg, S.L. (2009). How to map billions of short reads onto genomes. Nat Biotechnol *27*, 455-457.
Trapnell, C., Williams, B.A., Pertea, G., Mortazavi, A., Kwan, G., van Baren, M.J., Salzberg, S.L., Wold, B.J., and Pachter, L. (2010). Transcript assembly and quantification by RNA-Seq reveals unannotated transcripts and isoform switching during cell differentiation. Nat Biotechnol *28*, 511-515.
Wong, E.B., Khan, T.N., Mohan, C., and Rahman, Z.S. (2012). The Lupus-Prone NZM2410/NZW Strain-Derived Sle1b Sublocus Alters the Germinal Center Checkpoint in Female Mice in a B Cell-Intrinsic Manner. J Immunol *189*, 5667-5681.